Laser and Particle Beams (2009), *27*, 725–731.

doi:10.1017/S0263034609990504

Laser-produced plasma-wall interaction

O. RENNER,[1] R. LISKA,[2] AND F.B. ROSMEJ[3,4]

[1]Institute of Physics, Academy of Sciences of the Czech Republic, Prague, Czech Republic
[2]Czech Technical University in Prague, Faculty of Nuclear Sciences and Physical Engineering, Prague, Czech Republic
[3]Université Pierre et Marie Curie UPMC, LULI, UMR 7606, Paris, France
[4]École Polytechnique, LULI, PAPD, Palaiseau, France

(RECEIVED 30 August 2009; ACCEPTED 21 September 2009)

Abstract

Jets of laser–generated plasma represent a flexible and well-defined model environment for investigation of plasma interactions with solid surfaces (walls). The pilot experiments carried out on the iodine laser system (5–200 J, 0.44 μm, 0.25–0.3 ns, $<1\times10^{16}$ W/cm^2) at the PALS Research Centre in Prague are reported. Modification of macroscopic characteristics of the Al plasma jets produced at laser-irradiated double-foil Al/Mg targets is studied by high-resolution, high-dispersion X-ray spectroscopy. The spatially variable, complex satellite structure observed in emission spectra of the Al Lyα group proves a formation of rather cold dense plasma at the laser-exploded Al foil, an occurrence of the hot plasma between both foils and subsequent thermalization, deceleration and trapping of Al ions in the colliding plasma close to the Mg foil surface. The spectra interpretation based on the collisional-radiative code is complemented by 1D and 2D hydrodynamic modeling of the plasma expansion and interaction of counter-propagating Al/Mg plasmas. The obtained results demonstrate a potential of high resolution X-ray diagnostics in investigation of the laser-produced plasma–wall interactions.

Keywords: Dielectronic satellite line emission; Hydrodynamic plasma simulation; Laser-produced plasma; Plasma-wall interaction; X-ray spectroscopy

INTRODUCTION

Interactions of high-temperature plasmas with surfaces of solid materials (generally known as plasma-wall interactions, PWI) are extensively studied for their relevance to magnetic and inertial confinement fusion, primarily in the context of a development of future fusion reactors like ITER (Ikeda, 2007) or the fast ignitor scheme based HiPER (Dunne, 2006). Basic research directed at investigation of transient phenomena occurring near the surface of plasma-exposed materials is of paramount importance, as it contributes to an explanation of the PWI effects, provides data required for verification of advanced theoretical models, and new technological concepts needed to move from the scientific proof of the principle to a commercial reactor stage.

Laser-produced plasmas represent a very efficient tool for investigating plasma-solid interactions. A large span of interaction regimes available at nanosecond, picosecond, and femtosecond lasers (Gibbon & Förster, 1996) facilitates the realization of diverse PWI scenarios. By varying the parameters of laser-matter interaction (laser pulse energy, duration, focusing, target composition, and geometry), plasma beams with tailored particle distribution, energy and degree of collimation can be produced (Badziak *et al.*, 2007; Kasperczuk *et al.*, 2007; Laska *et al.*, 2008). The detailed information on environmental conditions in regions where the high-temperature plasma interacts with solids is typically obtained by optical (primarily infrared and visible) diagnosis (Gauthier *et al.*, 2005), by laser interferometry (Pisarczyk *et al.*, 2007), and by particle and X-ray diagnostic methods (Hauer *et al.*, 1991). Among the latter ones, applications of the high-resolution X-ray spectroscopy (Griem, 1997; Renner *et al.*, 2004) are particularly useful, as the complex analysis of the intense spectral line emission accompanying the plasma impact is generally the most efficient tool for visualizing the phenomena of PWI in the densest plasma regions opaque for optical probing.

The first experiments directed at laser-produced plasma-wall interaction (LPWI) defined the framework of the processes investigated (Mazing *et al.*, 1985; Beigman *et al.*, 1989; Shevelko *et al.*, 2001). When the plasma jets or intense radiation fluxes strike a solid surface (obstacle), the material is rapidly heated and partially ablated; an interplay

Address correspondence and reprint requests to: O. Renner, Institute of Physics of the AS CR, v.v.i., Na Slovance 2, 182 21 Prague 8, Czech Republic. E-mail: renner@fzu.cz

of attractive *versus* repulsive forces results in a formation of strong shock waves (Zel'dovich & Raizer, 2002). The elastic pressure (due to repulsive forces) becomes small in comparison with the thermal pressure, the compression, and consecutive unloading (rarefaction) waves induce a partial vaporization of the solid. The highly charged energetic ions approaching the obstacle interpenetrate the near-surface layer, collide with the counter-propagating matter, and capture a large number of electrons to high-lying atomic levels. The characteristics of the impinging plasma (density, temperature, charge, and excited states distribution) are strongly modified, material mixing phenomena result in radiative or three-body recombination, charge exchange (Rosmej *et al.*, 2006), and formation of hollow atoms (Rosmej & Lee, 2007).

Despite a huge progress in LPWI modeling, contemporary theoretical approaches, i.e., fluid hydrodynamic simulations, kinetic particle-in-cell approximations, or their hybrids (Evans, 2006), provide only qualitative predictions of the shock formation and the plasma evolution due to the complexity of the problems studied. Novel simulations based on an arbitrary Lagrangian Eulerian hydrocode (Liska *et al.*, 2008) generate promising results; however, their validity must still be experimentally confirmed.

Consequently, the acquisition of complex information on LPWI and, in particular, on processes involved in near-wall plasma collisions, depends mostly on the realization of well characterized experiments. The importance of such studies is emphasized by numerous weighty applications. In addition to the above-mentioned contribution to a construction of the future fusion reactors, knowledge of LPWI environmental conditions influences the design of sophisticated targets in indirect drive fusion schemes (Dittrich *et al.*, 1999), where different collisional scenarios between individual shells of fusion pellets and between blow-off plasma from inner walls of the hohlraum and the capsule occur. Stagnating and interpenetrating plasmas are frequently met in astrophysics and in laboratory experiments designed to model various astrophysical situations (Remington *et al.*, 2006 and references therein). Further applied problems include investigation of the energy dissipation and instability evolution in the plasmas (Berger, 1991), thermalization of the counter-streaming plasma plumes (Rancu *et al.*, 1995), etc.

Most of the previous experiments directed at the X-ray investigation of LPWI were performed with low-resolution instrumentation and with limited knowledge of interaction conditions. Here we report test-bed experiments with the colliding plasma clouds produced at single- or double-side laser-irradiated Al/Mg targets. This experimental configuration represents a well-defined model environment for studying PWI. The plasma interaction close to the Mg surface submitted to an energetic plasma jet is visualized *via* high-resolution X-ray spectroscopy. The satellite-rich structure observed in emission spectra of the Al Lyα group is interpreted using the atomic collisional-radiative code and discussed in terms of interaction of counter-propagating plasmas, in particular trapping, deceleration and thermalization of Al ions close to the Mg foil. One-dimensional (1D) and two-dimensional (2D) hydrodynamic modeling of the expanding plasma support the analysis of the observed spectra.

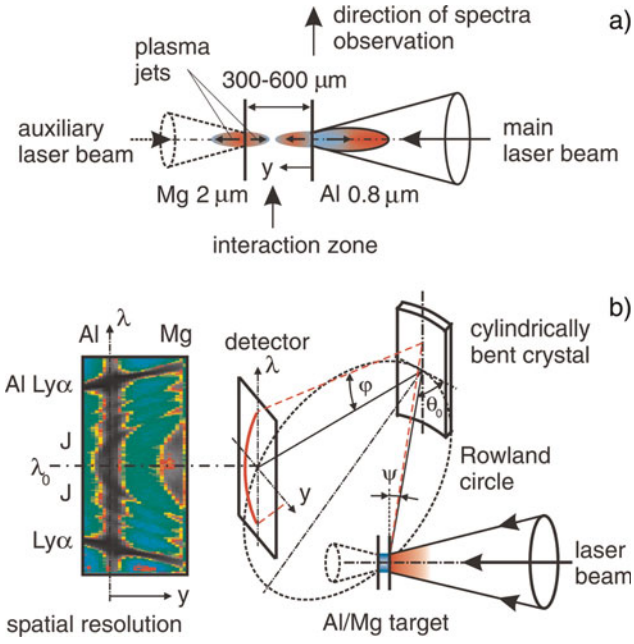

Fig. 1. (Color online) Scheme of the plasma formation at the laser-irradiated double-foil Al/Mg structure (**a**) and the experimental setup with the vertical dispersion Johann spectrometer (**b**).

PALS EXPERIMENT

The experiment was performed using the iodine laser system at the PALS Research Centre in Prague (Jungwirth *et al.*, 2001; Jungwirth, 2005). In accordance with Figure 1a, the double-foil targets consisting of two parallel foils of Al (thickness 0.8 μm) and Mg (thickness 2 μm) with a variable spacing were irradiated at normal incidence with one or two counter-propagating laser beams. The laser beams delivered 5–200 J of frequency-tripled radiation (0.44 μm) in a pulse length of 0.25–0.3 ns. Being focused to a diameter of 80 μm (main beam) or 50 μm (auxiliary beam), they yielded a maximum intensity of 1×10^{16} W/cm^2 on the target. Here we concentrate on the evaluation of two typical experimental configurations. In the first one, the data was obtained at foils separated by a distance of 360 μm and irradiated from the Al side only with the laser energy of 78 J. In the second one, the foils were separated by a distance of 600 μm and double side irradiated at 115 J (Al foil) and 6 J (Mg foil).

The diagnostic complex included optical spectroscopy, a pinhole camera coupled to a low-magnification X-ray streak camera, and a spherically bent mica crystal X-ray spectrometer (Rosmej *et al.*, 2006). The primary diagnostics was a vertical dispersion Johann spectrometer (VJS) fitted with a

crystal of quartz (100) cylindrically bent to a radius of 76.6 mm. As schematically shown in Figure 1b, the VJS disperses the radiation along a direction λ parallel to the axis of the cylindrically bent crystal, i.e., as a function of the vertical divergence angle φ. The instrument provides simultaneously two sets of 1D spatially resolved spectra symmetrically disposed about the central wavelength λ_0 (related *via* the Bragg equation to the angle θ_0); the existence of this axis of symmetry facilitates the computational reconstruction of the detected spectra. Due to the extremely high linear dispersion (~170 mm/Å), the VJS is characterized by the high spectral resolving power (close to 8000) and by the spatial resolution of 8 μm in a direction of the axis *y*. The raw spectroscopic data corresponding to the double-side laser-irradiated Al/Mg target with the inter-foil distance of 600 μm is shown in the insertion of Figure 1b. The wavelength coverage $\Delta\lambda/\lambda < 0.03$ is rather restricted but sufficient for a detailed observation of the Al Lyα group including the resonance line and its associated satellites. The time-integrated spectra were recorded on X-ray film and recalculated to the linear wavelength and intensity scale using an algorithm described by Renner *et al.* (1997). The reference transition Al XII $2p^2\ ^1D_2$-$1s2p\ ^1P_1$ (J-satellite with the wavelength of 7.2759 Å) used to calibrate the spectra was defined at the distance of 40 μm from the non-irradiated surface of the Al foil.

An example of the reconstructed spectrum is presented in Figure 2. This spectral emission from the single-side irradiated double-foil target was observed at an angle of $\psi = 0 \pm 0.8^\circ$, i.e., in the direction parallel to the Al foil surface. By using the tangential angle of observation, the spectra integration over strong plasma gradients perpendicular to the foil surface was avoided. An outer pair of the strongest spectral lines belongs to the Al Lyα doublet, the inner pairs of lines are identified as dielectronic satellites 2l2l' → 1s2l' with the J-satellite closest to the axis of symmetry. The satellite-rich structure observed at the non-irradiated (rear) surface of the Al foil gradually reduces to the emission of the Al Lyα only, although at 128 μm below the Al foil a weak J-satellite line can still be identified. In contrast to spectra recorded at single-foil Al target, where the observable Lyα and J-satellite emission extends up to 230 μm and 110 μm below the non-irradiated foil surface, respectively, the intensity of the resonance line emitted from the Al/Mg target below the Al foil approximately doubles, the Al Lyα emission is observable throughout the gap between both foils and the satellites reappear near the Mg foil. The intensity of the dominant J-satellite is comparable with that of the resonance transition. The discussion of this spectra behavior is provided in the next section.

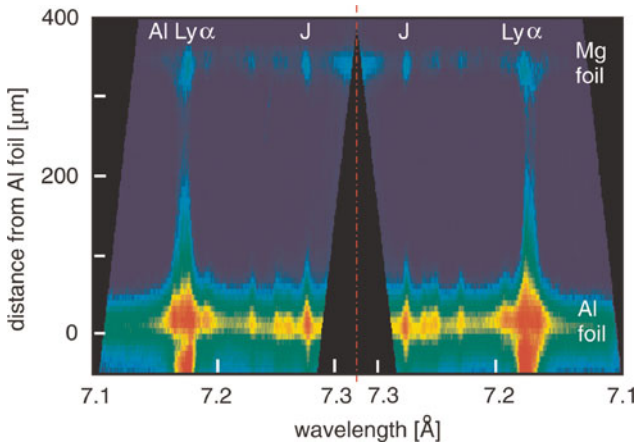

Fig. 2. (Color online) Spatially resolved spectra of the Al Lyα group recorded at single-side laser-irradiated Al/Mg target.

RESULTS AND DISCUSSION

A qualitative explanation of the observed spectral characteristics follows from 2D simulation of the plasma evolution performed using the Prague Arbitrary Lagrangian Eulerian hydrocode (PALE) (Kucharik *et al.*, 2006; Liska *et al.*, 2008). In this approach, after several steps of Lagrangian simulations, the deformed moving mesh is reconstructed and the conservative quantities are remapped (Eulerian part) on to a smoother grid. The hydrodynamics was based on a quotidian equation of state (QEOS), classical Spitzer-Harm model for the heat conductivity, and a simple approximation of the laser energy deposition at the critical density surface.

An example of the simulated distribution of the electron density n_e and temperature *T* corresponding to the double-foil Al/Mg target irradiated by the main laser beam only (78 J, 0.3 ns, 5×10^{15} W/cm^2) is shown in Figure 3. Here *r* is a polar axis of the used cylindrical coordinate system; its longitudinal axis *y* again coincides with the laser beam axis. The simulations indicate that the upper Al foil burns through before the laser pulse maximum, thus the Al ions are not trapped by the cold Mg foil but collide with the well

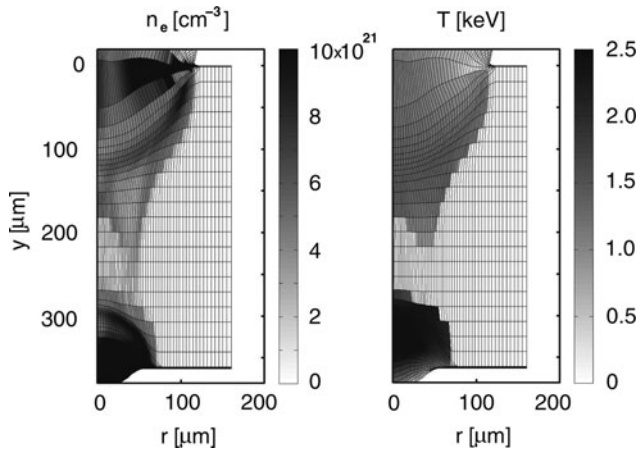

Fig. 3. Two-dimensional ALE code simulation of the colliding plasmas. The laser beam irradiates the upper Al foil from above, the Mg foil is positioned at the distance of $y = 360$ μm. The shown electron density and temperature distribution corresponds to the laser pulse maximum.

developed Mg plasma. A validity of this scenario is supported by the streak camera records demonstrating that a relatively strong emission from the plasma region close to the Mg foil appears before the intensively emitting Al ions reach the Mg surface (Renner *et al.*, 2007). A similar scenario, i.e., the plasma jets interaction with preplasma build-up at the secondary target due to the combined effects of the strong shock and rarefaction waves formation, scattered laser light, and intense plasma radiation (Morice *et al.*, 2008), should always be considered even if the residual laser energy does not directly strike the second foil. This means that the phenomena occurring in the near-wall region are to be interpreted in terms of the plasma collision, interpenetration, and ion trapping.

The environmental conditions in the plasma interaction zone were derived from the high-resolution spectra of the Al Lyα group recorded by the VJS. An analysis of the spectra shown in Figure 2 was performed by using the multilevel collisional-radiative code MARIA (Rosmej, 1997, 2001); the resonance doublet profile and its satellite structure were interpreted in terms of the macroscopic plasma characteristics. The main input parameters (electron density n_e, temperature T_e, the photon path length L, and differential plasma motion) were varied until the best fit between the experiment and simulation was achieved. The prospective overlap of the H- and He-like Mg ion emission with the Al Lyα spectra was checked by recording the emission from laser-irradiated single Al and Mg foils. The comparison of the spectra presented in Figure 4 suggests a possible interference of the Al Lyα and ^{1}S-satellite (satellites are grouped according to their final single excited states) with the Mg Heε and Heζ lines. Despite the contribution of the He-like Mg higher series members to the resulting spectra is rather weak, the neglect of the spectral lines overlap may result in the erroneous spectra interpretation. The model-independent decomposition of such composite spectra containing broadened line profiles with very close transition energies is frequently ambiguous (Adámek *et al.*, 2006), thus the diagnostic role of the non-disturbed J-satellite emission is of primary importance.

The detailed experimental spectra emitted from three characteristic plasma regions and their resulting fits are shown in Figure 5. The left- and right-hand side experimental spectra are well symmetric, this indicates an isotropic character of the plasma emission. The overall agreement between the synthesized and observed profiles is very good. The peak intensity of the J-satellite in the upper spectrum is overestimated due to lack of detailed width calculations of this satellite; however, its integral intensity is not substantially influenced. The plasma conditions corresponding to the Al Lyα group emission at the rear surface of the Al foil are characterized by the effective parameters $n_e = 3 \times 10^{21}$ cm^{-3}, $T_e = 300$ eV, and $L = 200$ μm. The Al line emission decreases monotonically with the distance from the Al foil. Between the foils, the satellite emission is suppressed and the effective plasma parameters at the mid-plane are characterized by electron densities of the level of 3×10^{20} cm^{-3} and temperatures above 700 eV. In the interaction region close to the Mg foil surface, the effects connected with the collision and interpenetration of counter-propagating plasmas are visualized *via* an increased emission of the Al Lyα line and its J-satellite. The plasma conditions at the Mg foil are best fitted by $n_e \sim (1-3) \times 10^{21}$ cm^{-3}, $T_e \sim 220$ eV, and $L = 500$ μm.

The area close to the Mg foil is of particular interest for studying the effects of the ion-wall interaction and plasma interpenetration phenomena. The presence of the Al emission near and below the Mg foil (Renner *et al.*, 2007) provides clear evidence of the plasma interpenetration. The increased integrated intensities and Doppler-broadened line widths of

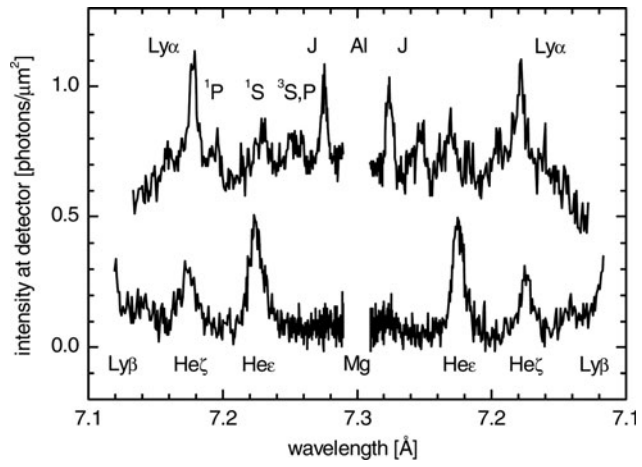

Fig. 4. Prospective overlap of the spectra emitted from the lase-explded Al and Mg foils.

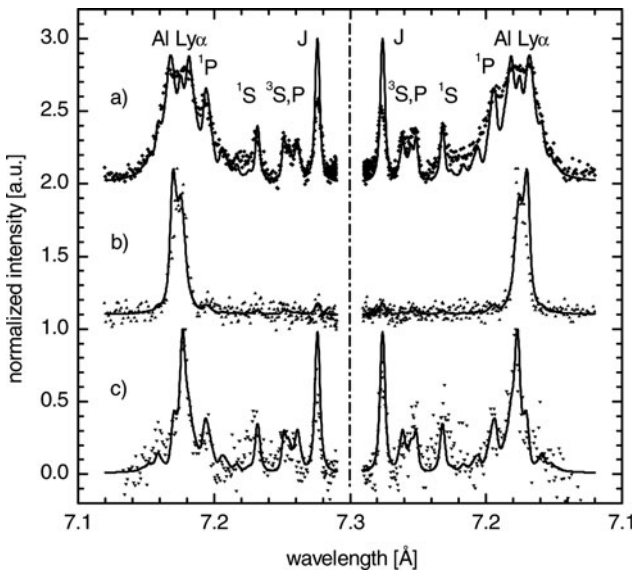

Fig. 5. MARIA code fitting (solid lines) of experimental Al Lyα spectra (points) observed close to the non-irradited surface of the Al foil (**a**), 128 μm below it (**b**), and at the Mg foil (**c**).

the Al Lyα emission (with the maximum observed at 40–60 μm above the Mg foil) consistently define the region of the density build-up and ion heating, i.e., the spatial range where collision and stagnation of the Al and Mg plasmas occurs. In addition to the intense plasma thermalization (conversion of the ion kinetic energy to thermal energy in a localized region), the gradual stopping of the Al ions in the counter-propagating Mg plasma is envisaged. Here we demonstrate the potential of high-resolution X-ray spectroscopy to measure precisely this ion deceleration *via* Doppler shifts of the emitted spectral lines.

These challenging measurements are conditioned by a proper choice of the experimental geometry and the investigated spectral transition. As mentioned before, the application of shallow angles ψ prevents the spectra integration over extended regions of plasma jets with strongly variable macroscopic parameters. On the other hand, this geometry results in sub-mÅ Doppler shifts due to 1D-ion velocity components directed normal to the target surface. Reliable identification of such small line shifts requires the application of high precision instruments like the VJS with its limiting precision of the relative wavelength measurements at the level of $(1-2)\times10^{-5}$ (Renner *et al.*, 1997).

The observations of the frequency shifts in the optically thick Al Lyα emission are affected by the radiation transfer effects, by the formation of higher-order satellites (Renner *et al.*, 2001) and by its overlap with the Mg Heζ line. In contrast, at given plasma parameters, the J-satellite is always optically thin. Calculations performed using the code FLYCHK (Chung *et al.*, 2005) indicate the J-satellite optical depth in the line center $\tau_0 = 0.5$ close to the Al surface and $\tau_0 \leq 0.4$ near the Mg foil. At these optical depths, the combination of the radial plasma expansion and radiation transfer effects should only result in symmetric broadening of the line profile. Therefore, the J-satellite represents a suitable candidate for the visualization of the Al ion stopping. Indeed, the analysis of the near-wall spectra shown in Figure 2 revealed almost monotonically decreasing red shifts of the Al J-satellite with the decreasing distance from the Mg foil. This J-satellite behavior agrees with the expected stopping of the Al ions at the Mg foil.

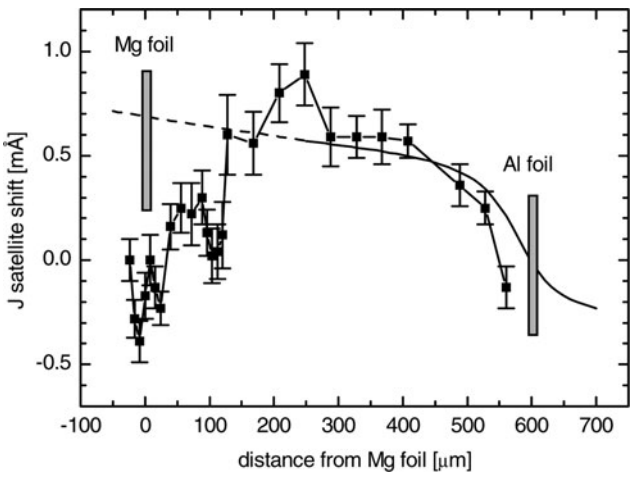

Fig. 6. Measured Doppler shifts of the J-satellite from the Al Lyα spectral group (points with error bars) and their comparison with theoretical predictions (solid and dashed line).

The more complicated dependence of the ion deceleration close to the wall was found in plasmas at the double-side irradiated Al/Mg targets. The environmental conditions in these colliding and interpenetrating plasmas depend on a direct energy deposition of both laser beams in Al and Mg foils (resulting in a creation of counter-streaming plasma plumes), on deposition of the laser energy scattered through both plasma clouds and on their mutual radiative heating. The current version of the PALE code with its simple one fluid multi-material approximation obviously cannot model all relevant processes in interpenetrating plasmas, however the more detailed simulations of the energy deposition are in progress.

The PALE 2D output data does not provide effective plasma characteristics relevant for time-integrated X-ray line emission at a given distance from the foil surfaces. In order to complete the scenario of the observed deceleration of the Al ions, the plasma evolution at single-side laser-irradiated Al foil was alternatively simulated by using the 1D hydrodynamics code MEDUSA supplemented by an average–atom model (Djaoui & Rose, 1992). The effective plasma characteristics were calculated by using the emission rate of the Al Lyα group as a weighing factor (Renner *et al.*, 1999). The validity of this simple 1D approximation for a detailed quantitative description of the 2D plasma expansion is limited, thus the obtained results are used only for a qualitative interpretation of the experimental data.

The plasma expansion at the two-side irradiated (115 J and 6 J, 0.3 ns, 7×10^{15} W/cm^2 and 1×10^{15} W/cm^2 at Al and Mg foil, respectively), 600-μm-spaced double-foil Al/Mg target was observed at an angle $\psi = 0.8^\circ$ in relation to the Al foil surface. Assuming that the Al ion expansion follows the MEDUSA predictions, then the expected Doppler shifts of the Al J-satellite emission are depicted by the solid line in Figure 6 (valid until the Al/Mg plasma collision area) and subsequently by the dashed line. The measured Doppler shifts are generally small but within their error bars, they agree well with the simulations. The prospective spurious effects introduced by the density- and temperature-dependent plasma polarization shifts are below the 0.1 mÅ level (Renner *et al.*, 2006). Starting from the inner Al foil surface, the J-satellite is stepwise shifted to red until a distance of about 250 μm from the Mg foil surface (the intense collision zone). After passing this distance, the Al ion deceleration reveals in the decreasing Doppler shifts. Assuming the gradual deceleration and simple trapping of the Al ions at the Mg surface, the J-satellite shift should monotonically decrease to zero. In contrast, the envelope of the observed Doppler shifts indeed tends to zero; however, their detailed spatial distribution exhibits distinct oscillations and even negative

values (blue shifts) which reflect the more complicated scenario of the ion deceleration including the ion back-scattering. The detailed interpretation of this phenomenon based on rigorous 2D description of interpenetrating plasmas and post-processing of hydrodynamic data is in progress.

CONCLUSION

We report the high-resolution X-ray measurements demonstrating the feasibility of spectroscopic investigation of laser-produced plasma-wall interactions. Using advanced methods of X-ray spectroscopy, the spectral line emission from the colliding plasmas produced at single- and double-side laser-irradiated Al/Mg targets was investigated. A detailed analysis of the complex dielectronic satellite structure in the Al Lyα group characterized the spatial distribution of the plasma parameters between inner surfaces of the target foils, their validity was supported by 1D and 2D hydrodynamic modeling. The unusual formation of Al spectra close to the Mg foil surface was explained in terms of thermalization and interpenetration of two colliding plasmas. The deceleration and trapping of Al ions at the Mg foil was studied *via* Doppler shifts of the J-satellite from the Al Lyα group, oscillations in the ion deceleration profile were discovered. The experimental configuration used provides a well-defined model environment for plasma interaction studies.

ACKNOWLEDGMENTS

This research was supported by the Czech Science Foundation Grant No. P205/10/0814, Ingo Grant No. LA08024, and the CNRS PICS project No. 4343. The experiments and their simulations were performed under the patronage of the Czech Ministry of Education, Youth, and Sports projects No. LC528 and 6840770022. The authors gratefully acknowledge the assistance of scientific and technical staffs from PALS in performing the experiments.

REFERENCES

Adámek, P., Renner, O., Drska, L., Rosmej, F.B. & Wyart, J.F. (2006). Genetic algorithms in spectroscopic diagnostics of hot dense plasmas. *Laser Part. Beams* **24**, 511–518.

Badziak, J., Kasperczuk, A., Parys, P., Pisarczyk, T., Rosiński, M., Ryc, L., Wołowski, J., Jablonski, S., Suchanska, R., Krousky, E., Láska, L., Mašek, K., Pfeifer, M., Ullschmied, J. & Dareshwar, L.J. (2007). Production of high–current heavy ion jets at the short–wavelength subnanosecond laser–solid interaction. *Appl. Phys. Lett.* **91**, 081502.

Beigman, I.L., Pirogovskiy, P.Ya., Presnyakov, L.P., Shevelko, A.P. & Uskov, D.B. (1989). Interaction of a laser-produced plasma with a solid surface: Soft X-ray spectroscopy of high-Z ions in a cool dense plasma. *J. Phys. B.* **22**, 2493–2502.

Berger, R.L., Albritton, J.R., Randall, C.J., Williams, E.A., Kruer, W.L., Langdon, A.B. & Hanna, C.J. (1991). Stopping and thermalization of interpenetrating plasma streams. *Phys. Fluids B* **3**, 3–12.

Chung, H.-K., Chen, M.H., Morgan, W.L., Ralchenko, Y. & Lee, R.W. (2005). FLYCHK: Generalized population kinetics and spectral model for rapid spectroscopic analysis of all elements. *High Energy Density Phys.* **1**, 3–12.

Djaoui, A., & Rose, S.J. (1992). Calculation of the time-dependent excitation and ionization in laser-produced plasma. *J. Phys. B* **25**, 2745–2762.

Dittrich, T.R., Haan, S.W., Marinak, M.M., Pollaine, S.M., Hinkel, D.E., Munro, D.H., Verdon, C.P., Strobel, G.L., McEachern, R., Cook, R.C., Roberts, C.C., Wilson, D.C., Bradley, P.A., Foreman, L.R. & Varnum, W.S. (1999). Review of indirect-drive ignition design options for the National Ignition Facility. *Phys. Plasmas* **6**, 2164–2170.

Dunne, M. (2006). A high–power laser fusion facility for Europe. *Nature Physics* **2**, 2–5.

Evans, R.G. (2006). Modelling short pulse, high intensity laser plasma interactions. *High Energy Density Phys.* **2**, 35–47.

Gauthier, E., Dumas, S., Matheus, J., Missirlian, M., Corre, Y., Nicolas, L., Yala, P., Coad, P., Andrew, P. & Cox, S. (2005). Thermal behaviour of redeposited layer under high heat flux exposure. *J. Nucl. Mat.* **337–339**, 960–964.

Gibbon, P. & Förster, E. (1996). Short-pulse laser-plasma interactions. *Plasma Phys. Contr. Fusion* **38**, 769–793.

Griem, H.R. (1997). *Principles of Plasma Spectroscopy.* Cambridge, UK: Cambridge Univ. Press.

Hauer, A.A., Delamater, N.D. & Koenig, Z.M. (1991). High-resolution X-ray spectroscopic diagnostics of laser-heated and ICF plasmas. *Laser Part. Beams* **9**, 3–48.

Ikeda, K. (2007). Progress in the ITER physics basis. *Nucl. Fusion* **47**, S1–S404.

Jungwirth, K., Cejnarova, A., Juha, L., Kralikova, B., Krasa, J., Krousky, E., Krupickova, P., Laska, L., Masek, K., Mocek, T., Pfeifer, M., Präg, A., Renner, O., Rohlena, K., Rus, B., Skala, J., Straka, P. & Ullschmied, J. (2001). The Prague Asterix Laser System PALS. *Phys. Plasmas* **8**, 2495–2501.

Jungwirth, K. (2005). Recent highlights of the PALS research program. *Laser Part. Beams* **23**, 177–182.

Kasperczuk, A., Pisarczyk, T., Borodziuk, S., Ullschmied, J., Krousky, E., Masek, K., Pfeifer, M., Rohlena, K., Skala, J. & Pisarczyk, P. (2007). Interferometric investigations of influence of target irradiation on the parameters of laser-produced plasma jets. *Laser Part. Beams* **25**, 425–433.

Kucharik, M., Limpouch, J. & Liska, R. (2006). Laser plasma simulations by Arbitrary Lagrangian Eulerian method. *J. Phys. IV France* **133**, 167–169.

Laska, L., Jungwirth, K., Krasa, J., Krousky, E., Pfeifer, M., Rohlena, K., Velyhan, A., Ullschmied, J., Gammino, S., Torrisi, L., Badziak, J., Parys, P., Rosinski, M., Ryc, L. & Wolowski, J. (2008). Angular distributions of ions emitted from laser plasma produced at various irradiation angles and laser intensities. *Laser Part. Beams* **26**, 555–565.

Liska, R., Limpouch, J., Kucharik, M. & Renner, O. (2008). Selected laser plasma simulations by ALE method. *J. Phys.* **112**, 022009.

Mazing, M.A., Pirogovskiy, P.Ya., Shevelko, A.P. & Presnyakov, L.P. (1985). Interaction of a laser-produced plasma with a solid surface. *Phys. Rev. A* **32**, 3695–3698.

Morice, O., Casanova, M., Loiseau, P., Teychenné, D. & Rousseaux, C. (2008). Nanosecond laser-plasma interaction studies in the context of the LIL facility. *J. Phys.* **112**, 022037.

Pisarczyk, T., Kasperczuk, A., Krousky, E., Masek, K., Miklaszewski, R., Nicolai, Ph., Pfeifer, M., Pisarczyk, P., Rohlena, K., Stenc, K., Skala, J., Tikhonchuk, V. & Ullschmied, J. (2007). The PALS iodine laser–driven jets. *Plasma Phys. Contr. Fusion* **49**, B611–B619.

Rancu, O., Renaudin, P., Chenais-Popovics, C., Kawagashi, H., Gauthier, J.-C., Dirksmöller, M., Missalla, T., Uschmann, I., Förster, E., Larroche, O., Peyrusse, O., Renner, O., Krouský, E., Pépin, H. & Shepard, T. (1995). Experimental evidence of interpenetration and high ion temperature in colliding plasmas. *Phys. Rev. Lett.* **75**, 3845–3848.

Remington, B.A., Drake, R.P. & Ryutov, D.D. (2006). Experimental astrophysics with high power lasers and Z pinches. *Rev. Mod. Phys.* **78**, 755–807.

Renner, O., Missalla, T., Sondhauss, P., Krousky, E., Förster, E., Chenais–Popovics, C. & Rancu, O. (1997). High-luminosity, high-resolution X-ray spectroscopy of laser-produced plasma by vertical-geometry Johann spectrometer. *Rev. Sci. Instr.* **68**, 2393–2403.

Renner, O., Sondhauss, P., Peyrusse, O., Krousky, E., Ramis, R., Eidmann, K. & Förster, E. (1999). High-resolution measurements of X-ray emission from dense quasi-1D plasma. *Laser Part. Beams* **17**, 364–375.

Renner, O., Rosmej, F.B., Krouský, E., Sondhauss, P., Kalachnikov, M.P., Nickles, P.V., Uschmann, I. & Förster, E. (2001). Aluminum Lyα group formation at high-intensity, high-energy laser-matter interaction. *J. Quant. Spectr. Rad. Trans.* **71**, 623–634.

Renner, O., Uschmann, I. & Förster, E. (2004). Diagnostic potential of advanced X-ray spectroscopy for investigation of hot dense plasmas. *Laser Part. Beams* **22**, 25–28.

Renner, O., Adámek, P., Angelo, P., Dalimier, E., Förster, E., Krouský, E., Rosmej, F.B. & Schott, R. (2006). Spectral line decomposition and frequency shifts in Al Heα group emission from laser produced plasmas. *J. Quant. Spectr. Rad. Trans.* **99**, 523–536.

Renner, O., Adámek, P., Dalimier, E., Delserieys, A., Krousky, E., Limpouch, J., Liska, R., Riley, D., Rosmej, F.B. & Schott, R. (2007). Spectroscopic characterization of ion collisions and trapping at laser irradiated double-foil targets. *Hi. Ener. Density Phys.* **3**, 211–217.

Rosmej, F.B. (1997). Hot electron X-ray diagnostics, *J. Phys. B.* **30**, L819–L828.

Rosmej, F.B. (2001). A new type of analytical model for complex radiation emission of hollow ions in fusion, laser and heavy-ion-beam-produced plasmas. *Europhys. Lett.* **55**, 472–478.

Rosmej, F.B., Lisitsa, V.S., Schott, R., Dalimier, E., Riley, D., Delserieys, A., Renner, O. & Krousky, E. (2006). Charge exchange driven X-ray emission from highly ionized plasma jets. *Europhys. Lett.* **76**, 815–821.

Rosmej, F.B. & Lee, R.W. (2007). Hollow ion emission driven by pulsed intense X-ray fields. *Europhys. Lett.* **77**, 24001.

Shevelko, A.P., Knight, L.V., Peatross, J.B. & Wang, Q. (2001). Structure and intensity of X-ray radiation in a laser plasma-wall interaction. *Proc. SPIE* **4505**, 171–178.

Zel'dovich, Ya.B. & Raizer, Yu.P. (2002). *Physics of Shock Waves and High-Temperature Hydrodynamic Phenomena*. Mineola, N.Y.: Dover Publications. 762–770.